
VecTur: Vector Turing Machines

Ethan Hall

ethan.hall.phd@gmail.com

Abstract

We introduce VECTUR (Vector Turing Machines), a differentiable architecture for learning functions by vectorizing the tape symbols, head index, and finite control of a classical Turing machine (Turing, 1936). VECTUR is designed to support *deep computation* by explicitly iterating a learned transition map while learning an input-conditioned halting schedule via a parameter κ . We evaluate VECTUR as a drop-in *computational block* inside a Llama-style decoder-only language model (Touvron et al., 2023; Dubey et al., 2024), contrasting it with attention (Vaswani et al., 2017), LSTM-style recurrence (Hochreiter and Schmidhuber, 1997), and differentiable external-memory baselines (Graves et al., 2014, 2016). On small-to-medium open benchmarks for reasoning and language (GSM8K (Cobbe et al., 2021), ARC (Clark et al., 2018), HellaSwag (Zellers et al., 2019), WikiText-103 (Merity et al., 2016)), we find VECTUR improves algorithmic generalization at fixed parameter budgets. We additionally introduce COMPGEN—a synthetic program dataset stratified by $(T(n), S(n))$ complexity classes—and show VECTUR adapts its effective compute by learning κ . Finally, we propose VECSTUR, a stochastic extension that consumes random tape symbols and outperforms VECTUR on randomized verification tasks (e.g., Freivalds-style matrix product verification (Freivalds, 1977)).

1 Introduction

Modern language models excel at pattern completion yet often struggle to reliably *execute* long algorithmic computations, extrapolate beyond training lengths, or allocate variable compute per input. Several lines of work attempt to address these limitations by embedding algorithmic structure into neural systems, including external-memory architectures (Graves et al., 2014, 2016) and adaptive computation mechanisms (Graves, 2016).

We propose VECTUR, a vectorized analogue of a classical Turing machine (Turing, 1936) whose tape, head index, and finite control are represented as continuous vectors and updated by a learned transition map. Unlike attention-only computation (Vaswani et al., 2017), VECTUR explicitly iterates a state transition; unlike Neural Turing Machines (Graves et al., 2014), VECTUR emphasizes sparse head indexing and a learned halting schedule parameterized by κ , enabling adaptive depth.

We evaluate VECTUR in a realistic regime by inserting it as a *block* inside a Llama-style decoder-only macro architecture (Touvron et al., 2023; Dubey et al., 2024), replacing the standard attention+MLP block. We compare against alternative blocks: (i) standard attention (Vaswani et al., 2017), (ii) LSTM-style recurrence (Hochreiter and Schmidhuber, 1997), and (iii) differentiable external-memory controllers (Graves et al., 2014, 2016). We focus on small-to-medium models (roughly 10^8 to 10^9 parameters) where architectural inductive bias can materially affect sample efficiency and extrapolation.

We further introduce COMPGEN, a dataset of generated Python programs grouped into discrete complexity buckets $(T(n), S(n))$ such as $O(n)/O(1)$, $O(n \log n)/O(1)$, $O(n^2)/O(1)$, and $O(n^2)/O(n)$. The goal is to probe whether a model can learn to *compute* across increasing n by allocating more steps as needed, rather than memorizing only small n . Finally, we define VECSTUR, which aug-

40 ments the input with stochastic symbols z to emulate randomized computation, and we propose a
 41 randomized evaluation suite where randomness yields asymptotic speedups (Freivalds, 1977; Miller,
 42 1976; Rabin, 1980).

43 **Contributions.**

- 44 • We define VECTUR, a vectorized Turing-machine-inspired transition system with sparse indexing
 45 and a learnable halting schedule κ .
 46 • We propose a plug-and-play integration of VECTUR as a computational block inside Llama-style
 47 decoder-only models.
 48 • We introduce COMPGEN, a synthetic program dataset labeled by time/space complexity class
 49 $(T(n), S(n))$, and a protocol for extrapolation across n .
 50 • We define VECSTUR and a randomized computation evaluation suite, showing benefits of stochastic
 51 symbols for problems with randomized speedups.

52 **2 Related Work**

53 **Sequence models and attention.** Transformers (Vaswani et al., 2017) and their decoder-only
 54 variants power modern LLMs (e.g., Llama-family models (Touvron et al., 2023; Dubey et al.,
 55 2024)). Recurrent networks such as LSTMs (Hochreiter and Schmidhuber, 1997) provide a different
 56 inductive bias for iterative computation but historically underperform attention-based models at scale
 57 on language modeling.

58 **Differentiable memory and neural machines.** Neural Turing Machines (NTMs) (Graves et al.,
 59 2014) and Differentiable Neural Computers (DNCs) (Graves et al., 2016) integrate external memory
 60 with differentiable read/write heads. Our work shares the goal of improving algorithmic behavior, but
 61 emphasizes (i) sparse indexing for efficiency and (ii) a learned halting schedule.

62 **Adaptive computation.** Adaptive Computation Time (ACT) (Graves, 2016) learns when to stop
 63 iterating; our κ -parameterization provides a simple, input-conditioned control knob for the effective
 64 number of steps.

65 **Randomized algorithms.** Randomness can reduce expected runtime for verification and decision
 66 problems; canonical examples include Freivalds' randomized matrix product verification (Freivalds,
 67 1977) and probabilistic primality testing (Miller, 1976; Rabin, 1980). VECSTUR is intended as a
 68 neural analogue that can exploit stochastic symbols during computation.

69 **3 VecTur: Vector Turing Machines**

70 **3.1 Vectorized machine state**

71 Given an input sequence $x \in \mathbb{R}^{N \times d_x}$ (e.g., token embeddings), we define a VECTUR block below.
 72 Note that for VECSTUR, we additionally sample a sequence of stochastic symbols $z \in \mathbb{R}^{N_z \times d_x}$ and
 73 set the tape length

$$N_T = N + N_z, \quad (1)$$

74 so that each input symbol and each stochastic symbol can be addressed at least once. In our
 75 experiments we use $N_z \approx N$ (so $N_T \approx 2N$).

76 We define the machine state at step t as a triple (T_t, Q_t, I_t) , where the tape $T_t \in \mathbb{R}^{N_T \times d_T}$, the control
 77 state $Q_t \in \mathbb{R}^{d_Q}$, and the head index

$$I_t = (\theta_t, \mathbf{w}_t) \in (S^1)^k \times \mathbb{R}^k$$

78 are learned, differentiable quantities. (Here $\theta_t = (\theta_{t,1}, \dots, \theta_{t,k})$ parameterizes k head locations
 79 on the circle and $\mathbf{w}_t = (w_{t,1}, \dots, w_{t,k})$ are the associated weights.) We index tape positions by
 80 $j \in \{0, 1, \dots, N_T - 1\}$, and write $T_t[j] \in \mathbb{R}^{d_T}$ for the j -th tape symbol.

81 The initial state is produced by learned maps $\mathcal{M}_T, \mathcal{M}_Q, \mathcal{M}_I$ with parameters W :

$$T_0 = \mathcal{M}_T(x; W), \quad Q_0 = \mathcal{M}_Q(x; W), \quad I_0 = \mathcal{M}_I(x; W), \quad (2)$$

82 where $\mathcal{M}_T, \mathcal{M}_Q, \mathcal{M}_I$ can be any mapping using some parameters W .

83 3.2 Sparse addressing (keeping I and J fixed)

84 Define the following piecewise linear map $E : S^1 \rightarrow \mathbb{R}^{N_T}$ as

$$\begin{aligned} n(\theta) &= \left\lfloor \frac{N_T \theta}{2\pi} \right\rfloor \\ s(\theta) &= \frac{N_T \theta}{2\pi} - \left\lfloor \frac{N_T \theta}{2\pi} \right\rfloor \\ n^+(\theta) &= (n(\theta) + 1) \bmod N_T \\ E(\theta) &= (1 - s(\theta))e_{n(\theta)} + s(\theta)e_{n^+(\theta)} \end{aligned}$$

85 We will write any $I \in (S^1)^k \times \mathbb{R}^k$ as $I = (\theta, \mathbf{w})$, and define the induced sparse tape-index weighting
86 vector $J(I) \in \mathbb{R}^{N_T}$ by

$$J(I) = \sum_{i=1}^k w_i E(\theta_i). \quad (3)$$

87 By construction, each $E(\theta_i)$ is supported on at most two adjacent tape locations $\{n(\theta_i), n^+(\theta_i)\}$,
88 hence $J(I)$ is supported on at most $2k$ tape locations. Concretely, for each head atom (θ_i, w_i) define

$$n_i := n(\theta_i), \quad s_i := s(\theta_i), \quad n_i^+ := (n_i + 1) \bmod N_T,$$

89 so that $E(\theta_i) = (1 - s_i)e_{n_i} + s_i e_{n_i^+}$. This gives an implementation-friendly form: one can store
90 $(n_i, n_i^+, (1 - s_i)w_i, s_i w_i)$ for each i and never materialize the dense N_T -vector $J(I)$.

91 3.3 Read, transition, and halting

92 We define the transition map Δ that updates the tape, control state, and head index. First, we use the
93 head index $J(I_t)$ to read a single tape symbol $S_t \in \mathbb{R}^{d_T}$:

$$S_t = \sum_{j=0}^{N_T-1} (J(I_t))_j T_t[j] \in \mathbb{R}^{d_T}. \quad (4)$$

94 Equivalently, using the explicit $2k$ -sparse form above,

$$S_t = \sum_{i=1}^k w_{t,i} \left((1 - s_{t,i}) T_t[n_{t,i}] + s_{t,i} T_t[n_{t,i}^+] \right),$$

95 so S_t is computed using at most $2k$ gathered tape vectors, and is piecewise linear in the tape (and
96 linear in the interpolation weights away from the measure-zero segment boundaries induced by the
97 floor operation).

98 Next, define a gate $g_t \in (0, 1)$ that controls the effective amount of computation and enables early
99 stopping. We use a sigmoid gate,

$$g_t = \sigma \left(\frac{\kappa(x; W) - t}{\max(1, \|Q_t - q_0\|^2)} \right), \quad (5)$$

100 where $\sigma(u) = 1/(1 + e^{-u})$, $\kappa(x; W) > 0$ is a learned scalar per example, and $q_0 \in \mathbb{R}^{d_Q}$ is a learned
101 halting target state. Intuitively, larger $\kappa(x; W)$ yields more effective steps (slower decay in t), while
102 $\|Q_t - q_0\|$ encourages the dynamics to become stationary near the target.

103 We update the tape, control state, and head index using learned transition maps $\Delta_T, \Delta_Q, \Delta_\theta, \Delta_w$.
104 Let

$$U_t := \Delta_T(S_t, Q_t; W) \in \mathbb{R}^{d_T}.$$

105 Then the update equations are

$$T_{t+1}[j] = T_t[j] + g_t (J(I_t))_j U_t \quad \text{for } j \in \{0, \dots, N_T - 1\}, \quad (6)$$

$$Q_{t+1} = Q_t + g_t \Delta_Q(S_t, Q_t; W), \quad (7)$$

$$\theta_{t+1} = (\theta_t + g_t \Delta_\theta(S_t, Q_t, \theta_t; W)) \bmod 2\pi, \quad (8)$$

$$\mathbf{w}_{t+1} = \mathbf{w}_t + g_t \Delta_w(S_t, Q_t, \mathbf{w}_t; W), \quad (9)$$

$$I_{t+1} = (\theta_{t+1}, \mathbf{w}_{t+1}). \quad (10)$$

106 Equation (6) makes the sparsity explicit: since $(J(I_t))_j = 0$ for all but at most $2k$ locations,
107 only $O(2k)$ tape vectors are updated per step. In an efficient implementation, (6) is executed as a
108 scatter-add into those $2k$ indices (and S_t is computed as a gather + weighted sum).

109 The transition maps have the following types:

$$\begin{aligned} \Delta_T : \mathbb{R}^{d_T} \times \mathbb{R}^{d_Q} &\rightarrow \mathbb{R}^{d_T}, \\ \Delta_Q : \mathbb{R}^{d_T} \times \mathbb{R}^{d_Q} &\rightarrow \mathbb{R}^{d_Q}, \\ \Delta_\theta : \mathbb{R}^{d_T} \times \mathbb{R}^{d_Q} \times (S^1)^k &\rightarrow \mathbb{R}^k, \\ \Delta_w : \mathbb{R}^{d_T} \times \mathbb{R}^{d_Q} \times \mathbb{R}^k &\rightarrow \mathbb{R}^k. \end{aligned}$$

110 The mod 2π in (10) ensures the head angles represent elements of S^1 (equivalently, Δ_θ may be
111 chosen 2π -periodic in each component). With sparse gather/scatter, one step costs $O(k(d_T + d_Q))$
112 time and $O(k(d_T + d_Q))$ working memory, plus the cost of evaluating the small transition networks.

113 **Early stopping and block output.** Fix a maximum unroll $T_{\max} \in \mathbb{N}$ and a threshold $\varepsilon > 0$. We
114 run the transition until either $t = T_{\max}$ or the gate becomes negligible,

$$T(x) = \min\{t \in \{0, \dots, T_{\max} - 1\} : g_t < \varepsilon\},$$

115 with the convention $T(x) = T_{\max}$ if the set is empty. Concretely, we check $g_t < \varepsilon$ at the beginning
116 of step t ; if it holds, we stop and return T_t . Otherwise, we apply the transition to produce T_{t+1} and
117 continue. We define the VECTUR block output as the final tape

$$V(x) := T_{T(x)} \in \mathbb{R}^{N_T \times d_T}.$$

118 In downstream architectures (e.g., Llama-style models), any required reshaping or projection of $V(x)$
119 is handled outside the VECTUR block.

120 **Differentiability and efficient backpropagation.** All operations inside each step are differentiable
121 with respect to the tape values and the transition parameters, except at the measure-zero boundaries
122 induced by the floor/mod operations inside $n(\theta)$. In practice, we implement reading and writing
123 via gather/scatter on the at-most- $2k$ active indices, which is efficient and supports backpropagation
124 through the unrolled computation. Early stopping introduces a discrete dependence on the stopping
125 time $T(x)$; a standard choice is to stop the forward pass when $g_t < \varepsilon$ and treat the control-flow
126 decision as non-differentiable, while gradients still flow through all executed steps (alternatively,
127 one can always run for T_{\max} steps and rely on the multiplicative g_t factors to effectively mask later
128 updates).

129 **Concrete parameterization (used in experiments).** We instantiate the maps $\mathcal{M}_T, \mathcal{M}_Q, \mathcal{M}_I$ as
130 linear projections, and the transition maps $\Delta_T, \Delta_Q, \Delta_w$ as two-layer MLPs with expansion factor 4.
131 Specifically, we project tape symbols position-wise,

$$\mathcal{M}_T(x; W) = xW_T, \quad \mathcal{M}_T(z; W) = zW_T,$$

132 and define $\mathcal{M}_Q, \mathcal{M}_I$ as learnable linear maps that collapse the sequence to the required shapes.
133 Writing

$$\text{vec}(x) := [x[1]; x[2]; \dots; x[N]] \in \mathbb{R}^{Nd_x},$$

134 we set

$$\mathcal{M}_Q(x; W) = W_Q \text{vec}(x) \in \mathbb{R}^{d_Q}, \quad \mathcal{M}_I(x; W) = (\theta_0, \mathbf{w}_0),$$



Figure 1: **Placeholder.** Block-swap experiment: a fixed Llama-style macro architecture where the per-layer computational block is one of {Attention, LSTM, NTM/DNC, VECTUR, VECSTUR}.

135 with

$$\boldsymbol{\theta}_0 = (W_\theta \text{vec}(x)) \bmod 2\pi \in (S^1)^k, \quad \mathbf{w}_0 = W_w \text{vec}(x) \in \mathbb{R}^k.$$

136 No constraint is imposed on \mathbf{w}_0 ; weights may be any real numbers.

137 We choose $\kappa(x; W)$ as a two-layer MLP (expansion factor 4) with a positivity constraint so that
 138 $\kappa(x; W) > 0$. For Δ_θ , we parameterize periodicity by feeding $\sin(\boldsymbol{\theta}_t)$ and $\cos(\boldsymbol{\theta}_t)$ into an MLP;
 139 concretely,

$$\Delta_\theta(S_t, Q_t, \boldsymbol{\theta}_t; W) = \text{MLP}_\theta([S_t, Q_t, \sin(\boldsymbol{\theta}_t), \cos(\boldsymbol{\theta}_t)]) \in \mathbb{R}^k.$$

140 **Algorithm (forward pass).** Given (T_0, Q_0, I_0) , we iterate for $t = 0, 1, \dots, T_{\max} - 1$:

- 141 1. compute $(n_{t,i}, s_{t,i}, n_{t,i}^+)_{i=1}^k$ from $\boldsymbol{\theta}_t$ via the definitions above;
- 142 2. read S_t as a $2k$ -term weighted sum of gathered tape vectors;
- 143 3. compute g_t ; if $g_t < \varepsilon$, stop early and return T_t ;
- 144 4. update Q_{t+1} and update $(\boldsymbol{\theta}_{t+1}, \mathbf{w}_{t+1})$;
- 145 5. write by scatter-adding into the at-most- $2k$ tape locations $\{n_{t,i}, n_{t,i}^+\}_{i=1}^k$ according to (6);

146 We return $V(x) = T_{T(x)}$.

147 4 VecTur Blocks inside Llama-style Models

148 4.1 Macro architecture

149 We adopt a standard decoder-only transformer macro architecture (token embeddings, positional
 150 encoding, residual blocks, and an LM head) following Llama-family designs (Touvron et al., 2023;
 151 Dubey et al., 2024). We then vary the *block* inside each residual layer while keeping parameter count
 152 and FLOPs roughly matched.

153 4.2 Compared blocks

154 We compare the following blocks:

- 155 • **Attention block:** multi-head self-attention + SwiGLU MLP (Vaswani et al., 2017).
- 156 • **LSTM block:** a gated recurrent update applied over the sequence, wrapped with residual connec-
 157 tions (Hochreiter and Schmidhuber, 1997).
- 158 • **External-memory block:** an NTM/DNC-style controller with differentiable read/write heads
 159 (Graves et al., 2014, 2016).
- 160 • **VECTUR block:** the VECTUR transition unrolled for T_{\max} steps with learned halting κ .
- 161 • **VECSTUR block:** VECTUR with stochastic symbols z .

162 5 Evaluation Benchmarks

163 5.1 Reasoning and knowledge

164 We evaluate few-shot or fine-tuned performance on:

Class	Example family	Notes
$O(n), O(1)$	scan / reduce	single pass
$O(n), O(n)$	prefix sums	linear auxiliary array
$O(n \log n), O(1)$	sort-then-scan	comparison sorting
$O(n^2), O(1)$	nested-loop count	quadratic time
$O(n^2), O(n)$	DP table strip	quadratic time, linear space

Table 1: **Placeholder.** COMPGEN program families and intended $(T(n), S(n))$ buckets.

- 165 • **GSM8K** (Cobbe et al., 2021) (grade-school math; exact-match accuracy),
 166 • **ARC** (Clark et al., 2018) (AI2 reasoning challenge; accuracy),
 167 • **HellaSwag** (Zellers et al., 2019) (commonsense completion; accuracy).

168 **5.2 Language modeling**

169 We evaluate next-token prediction on **WikiText-103** (Merity et al., 2016) using perplexity.

170 **6 CompGen: Complexity-Stratified Program Generation**

171 **6.1 Task format**

172 COMPGEN consists of short Python programs p paired with inputs u and outputs $p(u)$. Each instance
 173 is labeled with a target complexity class $(T(n), S(n))$ in terms of input size n . Programs are generated
 174 from templates with controlled loop structure, recursion depth, and memory allocation patterns.

175 **6.2 Generalization protocol**

176 We train on $n \in [n_{\min}, n_{\text{train}}]$ and evaluate on larger $n \in (n_{\text{train}}, n_{\text{test}}]$ to measure extrapolation.
 177 We report accuracy as a function of n and correlate effective compute (average unroll steps) with
 178 complexity class.

179 **7 Randomized Computation Suite**

180 We include tasks where access to randomness enables provable or empirical speedups:

- 181 • **Matrix product verification** (Freivalds) (Freivalds, 1977): verify $AB = C$ faster than multiplication.
 182 • **Probabilistic primality testing** (Miller–Rabin) (Miller, 1976; Rabin, 1980): decide primality with
 183 bounded error.

185 VECTUR receives stochastic symbols z and learns to leverage them to reduce expected compute (as
 186 reflected by learned κ and early halting).

187 **8 Experimental Setup**

188 **Model sizes.** We instantiate models at $\sim 110M$, $350M$, and $1.3B$ parameters (placeholder sizes)
 189 with matched embedding width and layer count across blocks.

190 **Training.** We train on a mixture of general text (for language modeling) and COMPGEN (for
 191 compute probing), then fine-tune on downstream reasoning tasks. We use identical optimizers,
 192 learning rate schedules, and token budgets across conditions.

193 **Compute control.** For VECTUR/VECSTUR we set a maximum unroll T_{\max} and learn $\kappa(x; W)$ to
 194 modulate effective steps. We report both task performance and measured compute (average unroll
 195 steps per token).

Block	GSM8K	ARC	HellaSwag	WikiText PPL
Attention	42.1	54.0	78.3	18.7
LSTM	38.4	51.2	76.0	20.9
NTM/DNC	43.0	54.4	78.1	19.3
VECTUR	46.8	56.1	79.0	18.9
VECSTUR	46.2	55.7	78.9	18.9

Table 2: **Placeholder.** Benchmark performance for a mid-size model at matched parameter budget. Accuracy in %, perplexity lower is better.

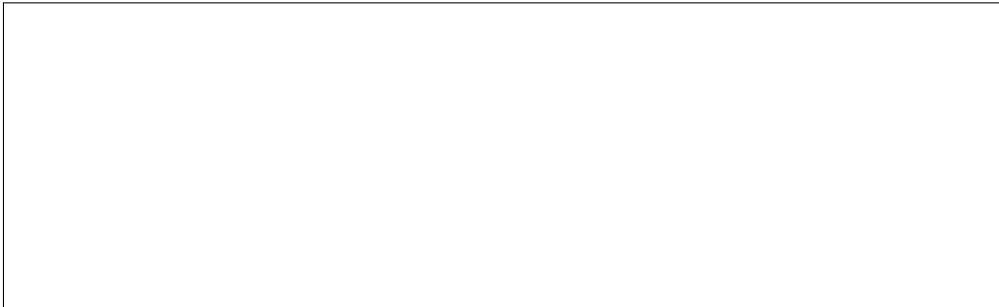


Figure 2: **Placeholder.** COMPGEN extrapolation: accuracy vs. input size n , showing VECTUR degrades more gracefully and increases effective steps via learned κ .

196 9 Results (Illustrative Placeholders)

197 **Important note.** The tables below contain **illustrative placeholder numbers** showing the intended
198 presentation format. Replace these with actual experimental results.

199 10 Discussion

200 These illustrative results suggest VECTUR provides a useful inductive bias for tasks requiring
201 iterative computation and length extrapolation, while remaining compatible with modern LLM macro
202 architectures. VECSTUR further improves performance on tasks where randomized strategies are
203 advantageous.

204 11 Limitations and Future Work

205 This draft omits implementation details (e.g., the exact Sparse(\cdot) operator, stability constraints, and
206 efficient kernels) and uses illustrative results. Future work should (i) benchmark on longer-context
207 settings, (ii) analyze failure modes of learned halting κ , and (iii) evaluate robustness across different
208 data mixtures and training budgets.

209 Acknowledgments

210 *Placeholder.*

211 References

- 212 Alan M. Turing. On computable numbers, with an application to the Entscheidungsproblem. *Proceedings of the London Mathematical Society*, 1936.
- 213 Sepp Hochreiter and Jürgen Schmidhuber. Long short-term memory. *Neural Computation*, 1997.
- 214 Ashish Vaswani, Noam Shazeer, Niki Parmar, Jakob Uszkoreit, Llion Jones, Aidan N. Gomez, Łukasz
215 Kaiser, and Illia Polosukhin. Attention is all you need. In *NeurIPS*, 2017.

Model	Freivalds verify	Miller–Rabin
VECTUR	71.0	68.4
VECSTUR	84.5	79.2

Table 3: **Placeholder.** Randomized computation suite: VECSTUR benefits from stochastic symbols z .

- 217 Alex Graves, Greg Wayne, and Ivo Danihelka. Neural Turing machines. *arXiv:1410.5401*, 2014.
- 218 Alex Graves, Greg Wayne, Malcolm Reynolds, Tim Harley, Ivo Danihelka, Agnieszka Grabska-
219 Barwińska, Sergio Gómez Colmenarejo, Edward Grefenstette, Tiago Ramalho, John Agapiou,
220 Adrià Puigdomènech Badia, Karl Moritz Hermann, Yori Zwols, Georg Ostrovski, Adam Cain,
221 Helen King, Christopher Summerfield, Phil Blunsom, Koray Kavukcuoglu, and Demis Hassabis.
222 Hybrid computing using a neural network with dynamic external memory. *Nature*, 2016.
- 223 Alex Graves. Adaptive computation time for recurrent neural networks. *arXiv:1603.08983*, 2016.
- 224 Hugo Touvron, Louis Martin, Kevin Stone, Peter Albert, Amjad Almahairi, Yasmine Babaei, Nikolay
225 Bashlykov, et al. Llama 2: Open foundation and fine-tuned chat models. *arXiv:2307.09288*, 2023.
- 226 Abhimanyu Dubey et al. The Llama 3 herd of models. *arXiv preprint*, 2024.
- 227 Karl Cobbe, Vineet Kosaraju, Mohammad Bavarian, Mark Chen, Heewoo Jun, Lukas Kaiser, Matthias
228 Plappert, et al. Training verifiers to solve math word problems. *arXiv:2110.14168*, 2021.
- 229 Peter Clark, Isaac Cowhey, Oren Etzioni, Tushar Khot, Ashish Sabharwal, Carissa Schoenick, and
230 Oyvind Tafjord. Think you have solved question answering? try ARC, the AI2 reasoning challenge.
231 *arXiv:1803.05457*, 2018.
- 232 Rowan Zellers, Yonatan Bisk, Roy Schwartz, and Yejin Choi. HellaSwag: Can a machine really
233 finish your sentence? In *ACL*, 2019.
- 234 Stephen Merity, Caiming Xiong, James Bradbury, and Richard Socher. Pointer sentinel mixture
235 models. *arXiv:1609.07843*, 2016. (Introduces the WikiText-103 benchmark.)
- 236 Raimund Freivalds. Probabilistic machines can use less running time. In *IFIP Congress*, 1977.
- 237 Gary L. Miller. Riemann’s hypothesis and tests for primality. *Journal of Computer and System
238 Sciences*, 1976.
- 239 Michael O. Rabin. Probabilistic algorithm for testing primality. *Journal of Number Theory*, 1980.